UNIVERSIDAD DE ANTIOQUIA

STRUCTURE-PROPERTY RELATIONSHIP OF PHOTO-CURABLE RESINS FOR 3D PRINTING

Author

León David Gil Olano

Universidad de Antioquia

Facultad de ingeniería, Departamento de Ingeniería Mecánica

Medellin, Colombia

2020

Structure-property relationship of photo-curable resins for 3D printing

León David Gil Olano

Research work presented as partial requirement to opt for the title of:

Mechanical Engineer

Mentor:

Prof. Henry Alonso Colorado Lopera, PhD

Research field:

Manufacturing and Engineering Materials

Research group:

Cements, Ceramics and Composites

CCComposites

Universidad de Antioquia

Facultad de ingeniería

Departamento de ingeniería Mecánica.

Medellín, Colombia

2020

Abstract

In this academic work the creation of a structure-property relationship of a photo-curable resin from Aycubic Company was sought. To achieve this, test specimens were design and printed with the Vat photopolymerization Additive Manufacturing technique, most widely known as 3D-printing of photo-curable resins. For the printing process of the test specimens a LCD printer was used. The PHOTON machine by Anycubic was advertised as a SLA apparatus (Stereolithography) and was available at the CCComposites 3D-printing laboratory. I managed to find out the optimum printing parameters and the influence of such parameters in the final mechanical properties of the final part. Not only were these parameters studied but also the post curing process. Traction tests were performed to acquire the strain and stress of the material.

By using statistical analysis and a Weibull distribution, the Weibull module regarding both strength data and strain data was obtained as well as the Strength vs strain curve. Moreover, the maximum effective resolution of the printer was determined by means of the design and printing of several micro structures in order to verify the feasibility of this technology for the creation of polymer matrix nanocomposites, and the possible insertion of carbon nanotubes (CNT's) and Copper nanoparticles (CNP's).

Key words: 3D-printing – micro structure – Stereolithography – UV resins – Additive Manufacturing

Resumen

En este trabajo se buscó crear la relación estructura-propiedades de las resinas foto curables de la compañía Anycubic, por medio del diseño e impresión de probetas y arreglos estructurales usando la técnica de impresión 3D por estereolitografía (SLA) con una máquina de procesamiento digital de luz (DLP-Digital Light Processing). Ésto con el propósito de determinar los parámetros óptimos de impresión y dimensionar el impacto de los mismos en las propiedades mecánicas de la pieza final. No solo se analizaron los parámetros de impresión, sino también el proceso de post-curado. Se realizaron ensayos de tracción a las probetas para obtener las gráficas de esfuerzo-deformación.

Por medio de un análisis estadístico y una distribución Weibull se hallaron dos módulos de Weibull, uno basado en esfuerzo y otro en la deformacion, así como la curva esfuerzo vs deformación del material. Adicionalmente se buscó determinar la resolución máxima efectiva de la impresora por medio del diseño e impresión de arreglos estructurales de diferentes tamaños con el fin de verificar la factibilidad de esta tecnología para la creación de nano compuestos de matriz polimérica, y la posible inserción de refuerzos de nano tubos de carbono y nano partículas de cobre.

Palabras clave: Impresión 3D – micro estructuras – Estereolitografía – resina – UV manufactura aditiva

Contents

1. Introduction

Additive manufacturing (AM), most frequently known as 3D-printing (3DP), is the process of creating parts with the addition of material layer by layer [1] to create a three dimensional model, opposite to conventional manufacturing in which such material is removed to create the desired part. Therefore, 3DP reduces the consumption of raw material which in turn can decrease the manufacturing costs [2]. AM is divided into seven categories by the ASTM standard, which are: vat photopolymerization, binder jetting, directed energy deposition, material extrusion, material jetting, powder bed fusion, and sheet lamination [3]. 3D-printed parts are usually used for rapid prototyping and the number of end-use 3D-printed parts have been increasing lately, however, a study [4] from more than 100 industries in the United States showed that there is a small group of manufacturers using AM for the production of their final products.

The vat photopolymerization (VP) ASTM category consists in a number of manufacturing techniques using light as a stimulus to start a focused polymerization reaction. One of the most representative features of vat photopolymerization techniques is that it possesses the highest resolution and surface finish of all AM processes [2]. The main drawback of VP resides on the feedstock materials, as the polymer to be used has to be a resin that can start its cross-linking process by means of light, known as photo-curable resins, which constraints the application of this technology. There are two exposures techniques in VP: serial scanning and flood exposure. Serial scanning works by running a laser over the resin to selectively polymerize the resin, while flood exposure selectively casts light on the layer according to the cross section of the part to polymerize the resin [2]. Stereolithography (SLA) being a Serial scanning technique and Digital light processing (DLP) being a flood exposure technique.

Figure 1. Resolution difference between SLA and DLP technologies. Taken from [5].

SLA uses a laser to cure selectively the polymer through the action of scanning mirrors, sometimes lenses are used to help focus the laser light. This process can achieve a final print resolution of 20 μm [6], this resolution is related to the laser beam size. A common set up of SLA technology is depicted in **Figure 2**. On the other hand, DLP relies on a digital micro-mirror device used in order to project different light geometries of the part cross section, to polymerize a complete layer of resin, making this process faster (but sacrificing resolution), as the minimal measure of the final printed part is limited by the pixel size of the projector screen. A common set up of DLP technology is shown in **Figure 2.**

As a result of the differences in the operating conditions and apparatus set up, SLA technology offers a more accurate impression with a very high resolution (***Figure 1***), but it takes longer than DLP, as DLP can print complete layers at a time its printing times are considerably shorter. The pixelated effect on the DLP technology is due to the light being projected from a light projector, the pixel size determines the accuracy of each printing. Such pixel size is usually referred to as a "voxel" in 3D printing [7], which is considered short for "Volumetric picture element" or "volumetric pixel".

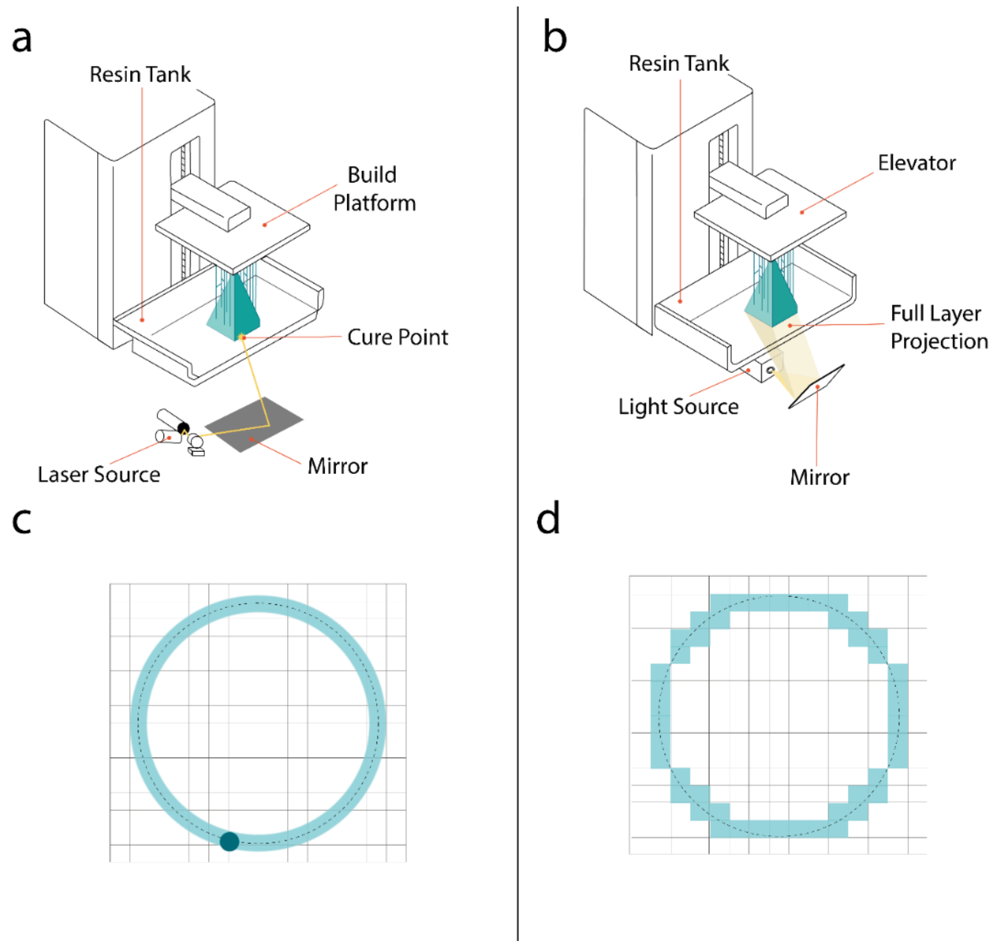

Figure 2. SLA vs DLP technologies. a) SLA apparatus set up. b) DLP apparatus set up. c) Laser beam sized resolution from SLA, in which a single point gets cured at a time without a pixelated effect. d) Display pixelated resolution from DLP, in which a complete projected geometry (layer) gets cured.

The purpose of creating composite materials is to take advantage of useful properties of different materials while trying to limit their particular drawbacks. Using Nano metric materials as reinforcement for the resin matrix in SLA and DLP manufacturing processes can significantly increase the properties of the final nanocomposite [8]. This mixing of Nanocomposites with the VP techniques has led to a new research field which has involved multiple kinds of applications such as radar absorbing materials [9], piezo electric materials [10], biomedical [11], printable elastic conductors [12], hydrogels [13], among others.

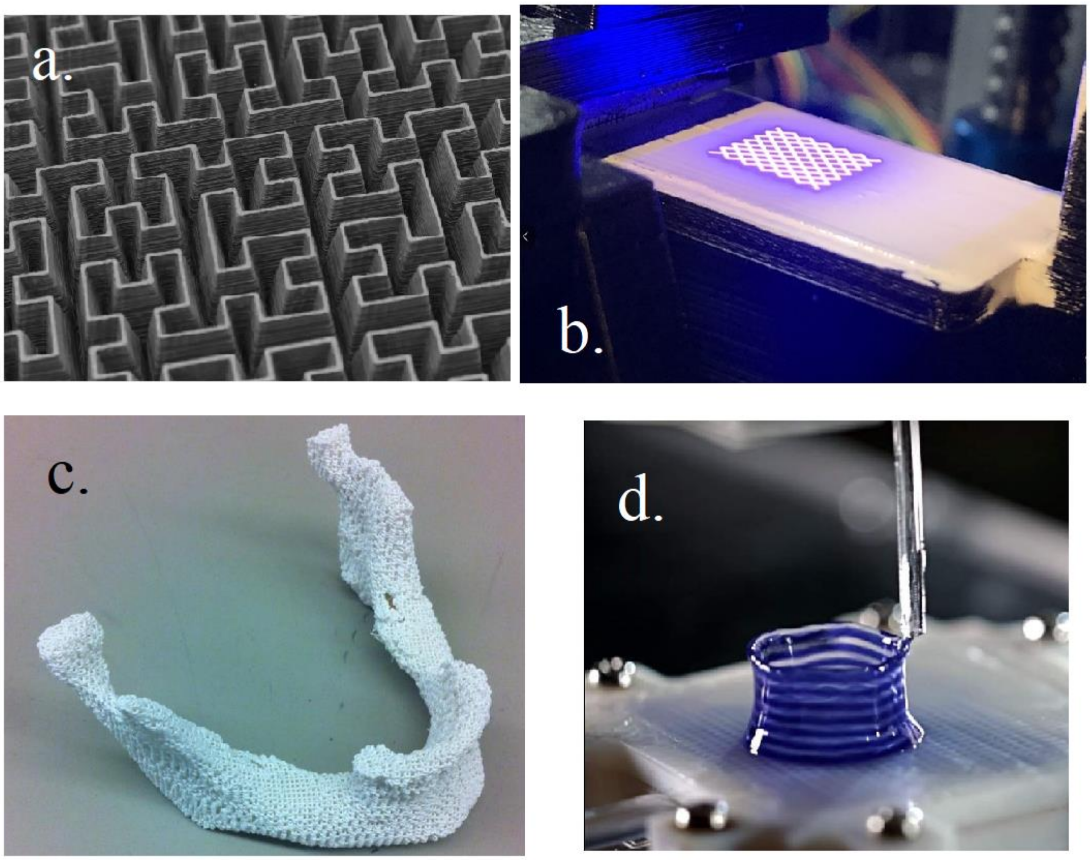

Figure 3. Some 3DP applications. a) RF absorbing 3D printed material [14]. b) 3D printed piezoelectric [15]. c) 3D printed bone scaffold [16]. d) 3D printed hydrogel [17].

The resin used for this academic work was supplied by Anycubic, which started as a company dedicated to selling components for DIY 3D printers. In 2015 Mr. James Ouyang co-founded the company as we know it today, and make Anycubic one of the most famous and reliable companies that manufactures and distributes all kind of components regarding 3D printing, from basic FDM machines to sophisticated SLA apparatuses and post curing machines. Not only does the company sell this kind of devices, but also supplies all kind of filaments and resins for photo-curable processes [18].

2. Objectives

2.1. General objective

Study the structural properties of photo curable resins exposed to UV curing processes under Stereolithography techniques (SLA 3D printing) by using the Photon Anycubic SLA apparatus.

2.2. Specific objectives

- Determine the optimal printing parameters for the requires printing conditions, including parameters such as UV exposure time and layer thickness.
- Design and manufacture test specimens to acquire mechanical properties of the cured resin.
- Design a statistical data processing to acquire the relevance of the printing parameters involved in the photo-curing process of resins for 3D printing.

3. State of the art

In order to obtain relevant and precise information on the topic, a systematic review on the SLA and DLP technologies was performed. Not only basic information about the processes was acquired, also an economical and life cycle assessment approach was addressed.

The information obtained in this state of the art was obtained by using the Scopus database as a reliable academic source of information that Universidad de Antioquia has made available for its undergraduate and postgraduate community.

3.1. Systematic bibliographic review

As the aim of this study is to analyze those articles relating nanocomposite materials and the VP technologies, an initial search in the database was performed involving the "nanocomposite" and "additive" topics. Searches were narrowed by excluding publications before 2015 which were surprisingly very few [13–16]. Also, books and book chapters, as well as conference papers, were excluded from the search as this review will only analyze research articles. The search was conducted using the search strings and keywords listed in Table 1.

Table 1. Search strings, keywords, terms and combined terms of the systematic search.

Search string / keywords	
Terms	Nanocomposites, 3Dprinting, AM, SLA, DLP, costs, LCA
Combined terms	VAT photopolymerization, circular economy, life cycle assessment
Search String 1	ALL (nanocomposites)) AND (((additive)) AND (sla)
Search string 2	ALL (nanocomposites)) AND (((additive)) AND (sla) AND (cost)
Search string 3	ALL ((nanocomposites) AND ((sla) OR (stereolithography)) AND ("life cycle"))

Figure 4 shows the Scopus report on the number of articles by country (the 10 most relevant countries) in the study of the 137 initial results of the search string 1, with the United States and China taking participation in over 30 documents each, followed by India and the United kingdom with nearly half the participation from that of the United States and China individually.

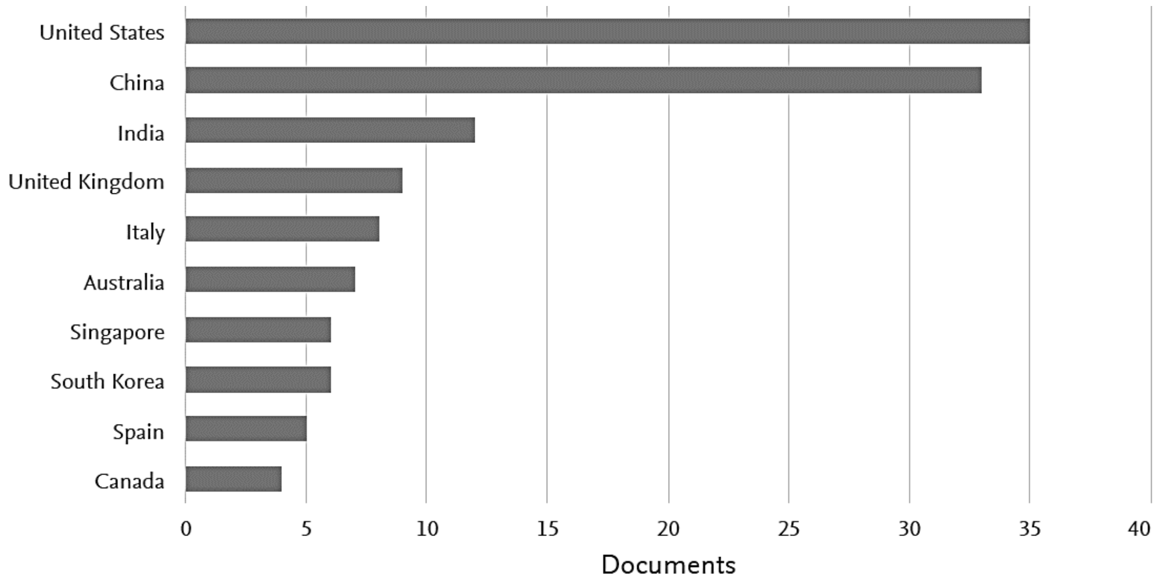

Figure 4. Number of articles in the VAT-photopolymerization techniques by country.

Each search string was filtered two times in order to narrow the number of articles in each search by relevance in the field of study. **Table 2** shows the number of articles per search and its subsequent filtering stages. The first filter applied in all the searches was a Scopus database automatic filter of the publish year, the search was narrowed down to articles excluding articles before 2005, in this initial filter stage only research articles were kept. The second filtering stage was an extensive look up at the title, abstract and keywords of each paper so articles not referring to nanocomposites obtained by VAT photopolymerization were excluded in order to ensure the relevance of the final documents.

Table 2. Number of results in the Scopus database for each search string and their subsequent filtering stages.

Search string	# of results	Filter 1	Filter 2
ALL (nanocomposites)) AND ((additive) AND ("sla")	137	122	16
ALL ("stereolithography")) AND ("nanocomposite") AND (cost)	45	41	4
ALL ((nanocomposites) AND ((sla) OR (stereolithography)) AND ("life cycle"))	35	24	5

After a detailed analysis of the results obtained in the second filter of search string 1 the number of articles selected for the first part of the study on the nanocomposites obtained by VAT-photopolymerization techniques was narrowed down to a total of 10 documents.

3.1.1. VAT photopolymerization.

This first stage of the study focused on the analysis of the results obtained in the first search string after the filtering stages. The final 10 documents selected for this first stage will be discussed and the results were classified into 5 different areas (graphite Nano-composites, biomedical, Nano cellulose, Nano-particles, and Nano-structures using the VAT photopolymerization 3D printing techniques. **Table 3** presents the journals in which the selected articles appeared as well as their main area of impact and year of publication. The number of articles per publication year is represented in **Figure 6**, and the number of selected articles by area of application with its corresponding percentage of participation is represented in **Figure 5**.

Table 3. List of selected articles for the VAT-photopolymerization stage of the systematic review with their corresponding publication year, journal and main area of impact.

ref	year	journal	main area
[23]	2020	Polymers MDPI	graphite Nano-composites
[24]	2020	Materials Science and Engineering R: Reports	biomedical
[25]	2020	Journal of Applied Polymer Science	Nano cellulose
[26]	2019	ACS Applied Materials and Interfaces	graphite Nano-composites
[27]	2019	Nanomaterials MDPI	Nano cellulose
[28]	2019	Composites Part B: Engineering	graphite Nano-composites
[29]	2018	Polymers MDPI	Nano-particles
[30]	2017	ACS Applied Materials and Interfaces	graphite Nano-composites
[31]	2017	ACS Applied Materials and Interfaces	Nano cellulose
[32]	2015	Polymers for Advanced Technologies	biomedical

All of the 10 articles selected in this first stage had a deep insight of the VAT photopolymerization technique which is defined as the layer by layer additive manufacturing process in which a light stimulus initiates a focused polymerization reaction on a photo sensitive resin.

3.1.2. Stereolithography (SLA)

The stereolithography 3D printing technique (usually referred to as SLA) consists on the curing of a specific point of a layer of the part to be printed, this is usually obtained by means of a focused laser beam, thus the final resolution of the printed part is the size of the beam itself. **Figure 2** shows a schematic set up of a SLA device.

Table 4 shows the studies in which a SLA apparatus was used, along with the kind of printer used and the main improved feature with the addition of the nano-filler.

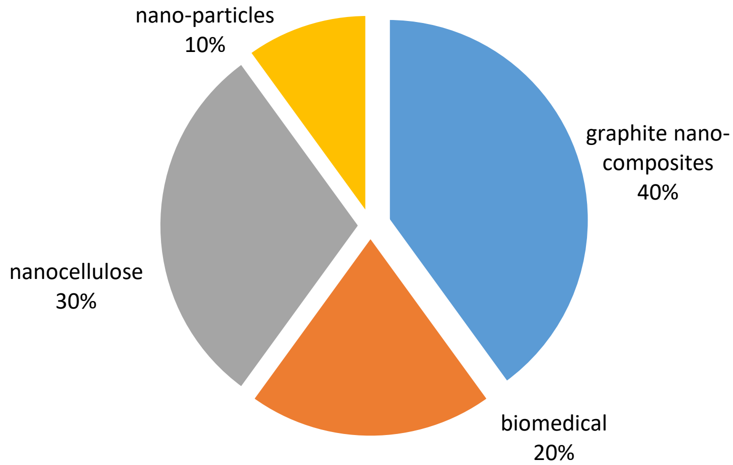

***Figure 5**. Participation in the Stage 1 of the study by area of application.*

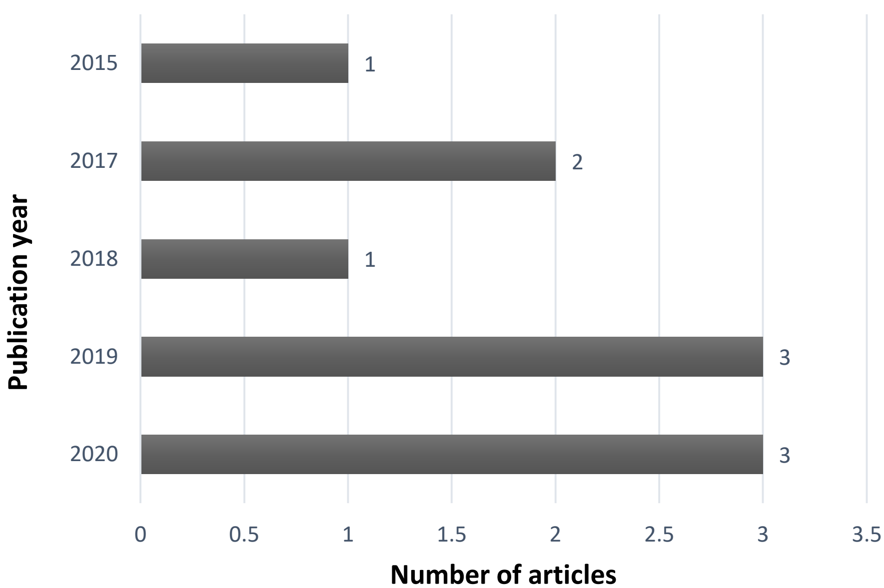

Figure 6. Number of articles per publication year.

Table 4. Articles that used a SLA apparatus.

ref	printer	technique	improved features
[17,23]	Form 1+	SLA	stiffness, tensile strength, thermal conductivity
[24]	NR	SLA	Continuous printing
[25]	Autocera	SLA	Tensile strength, modulus
[19,22,24]	Form 2	SLA	Tensile strength, ductility

3.1.3. Digital light processing (DLP)

The digital light processing 3D printing technique (usually referred to as DLP) consists on the curing of an entire layer of the part to be printed. This is usually achieved by using either a UV display or a UV light projector, which projects the geometry of a complete layer at the same time, thus achieving faster printing times but reducing the resolution of the print, as such resolution is now the pixel size of the screen or projector. **Figure 2** shows a schematic set up of a DLP device. **Table 5** shows the studies in which a DLP apparatus was used, along with the kind of printer used and the main improved feature with the addition of the Nano reinforcement.

Table 5. Articles that used a DLP printing technology.

ref	printer	technique	improved features
[27]	Duplicator D7 +	DLP	Tensile strength
[32]	Envisiontec Perfactory3	DLP	Tensile strength, E Modulus, toughness
[28]	Autodesk 3ds Max	DLP	compression stress

3.1.4. Materials

In this section the different materials used throughout the 10 articles will be listed (**Table 13**), as well as enhancements in properties achieved by both of the Vat photopolymerization techniques. The materials used were classified into matrix materials and Nano-reinforcements. **Figure 7** shows the different types of Nano-reinforcements used in the studies with its corresponding participation.

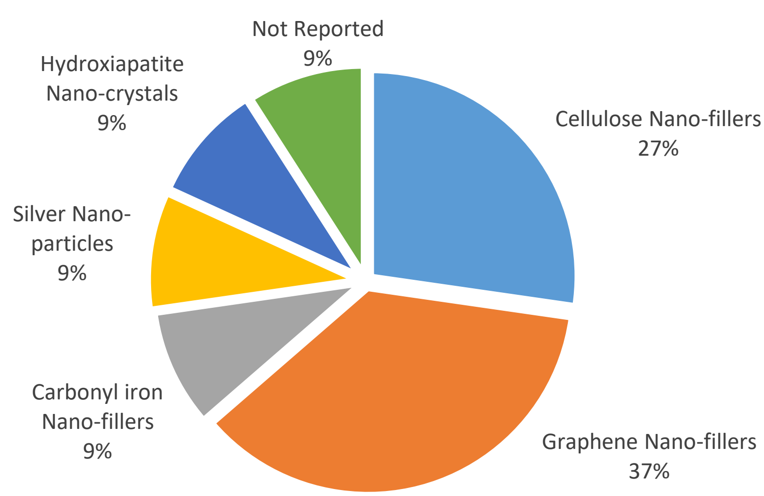

Figure 7. Nano-fillers used with its corresponding percentage participation in the articles.

All of the studies used nano-sized particles to reinforce the polymeric matrixes. Most of the studies used an acrylic or methacrylic acid resin [18,20-25], while only 3 of the studies used a custom mixture of resins to achieve their final nanocomposite matrix [19,26,27]. J. O. Palaganas *et al*. and J. Z. Manapat *et al*. did not purchase a commercial nano-reinforcement, instead, they both synthetized graphene oxide (GO) and obtained these nano particles through laboratory-controlled chemical reactions and then freezing and grinding the resulting GO material to obtain the end-use nano GO.

3.1.5. Pre processing

In the field of nanocomposites obtained by Vat-photopolymerization, a wide range of preprocessing techniques is usually required to ensure the dispersion of the reinforcements within the resin. This can be reflected on the selected documents as all of them required a sort of preprocessing technique, from simple mechanical stirring to complex surface abrasion of the Nano-fillers.

Mixing the resin and the Nano-fillers is a crucial preprocessing step to homogeneously disperse the reinforcement into the resin and avoid agglomeration of fillers [2], as this will result in uncured or partially cured spots. Three of the studied articles used sonication [18,23,24] as mixing method, some others focused on performing a surface abrasion or treatment of the nanoparticles to assure a proper matrix-reinforcement bonding [20,21,23,25], as some particles may show hydrophobic properties which decrease the successful addition of the Nano fillers. All of the different pre-processing strategies used in the analyzed articles are shown in **Table 13**.

3.1.6. Post processing

Both of the Vat-photopolymerization techniques studied in this review produce a semi green part, which means that there is no complete reaction of the cross-linked photopolymerization thus generating a mandatory post-processing, requiring both a cleaning wash for uncured resin leftovers [33] and a post curing process to ensure the full reaction in the end nanocomposite. All of the articles analyzed in this study used either of the before mentioned post treatments, some of them even using a heating process during or after the post curing process. All of the post cured parts in the articles used either thermal [34] or UV [35] final cure of the nanocomposite. **Figure 8** shows a post-curing UV machine to solidify the printed parts.

Figure 8. UV post-cure machine [36].

Five of the ten articles reported de use of Isopropyl alcohol (IPA) to wash out the remains of uncured resin [17,19,20,22,23]. At the same time most of them used a thermal curing, as heat is known to emit light in the non-visible spectrum, so ovens were used to finish the curing process in 5 of the studies [17,18,19, 22,23]. In addition, there were several documents that reported the use of UV post curing machines [17,18,19,21] to ensure the complete curing of the end parts. Two of the studies reported the use of Ethanol to wash out the uncured resin leftovers [22,26] instead of the usual IPA wash.

3.1.7. Cost Analysis

The search string 2, which was a refined search of the articles that related the VAT-photopolymerization techniques with the word "costs", initially returned 45 results, however, most of the results did not actually state cost related information. Most of them just mentioned the word "cost" in terms like "low cost", "high costs", and alike. So this second stage study will only focus on 4 articles considered relevant for the cost Analysis. **Table 6** references these documents with their corresponding publication year, journal and country.

Table 6. Cost related articles with their corresponding country, Journal and publication year.

ref	Pub year	Journal	Country
[37]	2020	Nanomaterials NDPI	China
[38]	2020	Progress in Materials Science	United States
[39]	2019	Journal of Nanomaterials	China
[40]	2018	Additive Manufacturing	United States

In this section of the systematic review 2 important topics were identified to be analyzed, which were both the technology and Material costs.

3.1.8. Technology costs

There are many technology suppliers involved in the process of additive manufacturing of nanocomposites. The documents analyzed in this section did not present the purchase costs of their printing devices. Though all of them mentioned the word "cost". None of them showed an interest in the economic aspects of the producing of their nanocomposite materials obtained by VP. **Table *7*** shows a list of the printing devices used in the documents from search string 1, 2 and 3 with corresponding used VP technique, device purchase cost range, and their main features of dimensions and power.

S. Mubarak *et al.* [41], as well as Feng, Zuying *et al.* [39] insisted that VP technologies were considered low cost AM techniques, in contrast J. Dizon *et al.* [40] mentions SLA techniques as being high energy consuming due to the usage of lasers that results into high heat losses, which is indirectly converted into money loss. Wu, H. *et al.* referred to VP produced parts as being "cost-effective", and emphasizing on the importance of this factor for hearing aids, orthopedics and prosthetics, and surgical guides and models [42].

Table 7. Technology cost of various apparatuses used in the study. NF: Not Found.

ref	Device	Type	Dimensions/Power	Cost range (USD)	Source
[27]	Duplicator D7 +	DLP	**Build Volume:** 120 x 68 x 180mm **Power: 48 W**	700 - 1,000	[43]
[32]	Envisiontec Perfactory 3	DLP	**Size:** 73 x 48 x 135 cm **XY accuracy:** 0,05 mm	50,000 - 110,000	[44]
[17,23]	Form 1 +	SLA	**Dimensions:** 30 × 28 × 45 cm **Power:** 60 W	3,299 - 3,600	[45][46]
[19,22,24]	form 2	SLA	**Dimensions:** 34.5 × 56 × 79 cm **Power:** 65 W	3,500 - 4,000	[47]
[39]	Photon	SLA	Printing volume : 115 x65x155 **Power :** 40W	230 - 300	[48]
[37]	Dream 3D-C200	SLA	NF	NF	NF

3.1.9. Material costs

None of the 19 articles from this study presented any sort of material purchase costs, nor compared costs of either the resins or the reinforcements.

3.1.10. Life cycle assessment (LCA)

On this third stage of the study, articles that related VP technologies, nanocomposites and Life cycle assessment were of interest. 35 articles were initially scouted by the Scopus database, after their subsequent filtering and analysis of abstract, title, and keywords. Only 5 articles out of the initial 35 documents mentioned the compound term of "life cycle assessment" or LCA. LCA is a technique used to evaluate the potential environmental impact of a product life cycle starting from the raw materials involved in its fabrication, to the final product and disposal [49].

Table 8. Environmental and LCA related articles.

ref	Year	Journal	Area of impact
[50]	2017	Advanced Science	energy
[13]	2019	Chemical Engineering Journal	degradation
[51]	2019	Journal of Water Process Engineering	water quality
[52]	2020	Chemical Engineering Research and Design	air quality
[53]	2020	Applied Materials Today	waste, energy, air quality

Diagrams showing general LCA processes were shown [52]. LCA of 4D printed parts with VP techniques was commented by Prasansha Rastogi, Balasubramanian Kandasubramanian [13]. In some studies, the term LCA was not used, and a LCA was not considered, however, they discussed the production of VP printed parts for environmental purposes [42,43], which related the final printed parts directly to the life cycle of such technologies.

Khosravani, M.R. *et al.* [53], studied the LCA of various AM techniques, including SLA. They manifested their concerns about the environmental impact of SLA technology due to the high energy consumption from this technology compared to other more environmentally friendly AM techniques. **Table 8** shows the articles studied in this third stage classified by their area of environmental impact.

4. Methodology

This academic work focused on obtaining a reliable and accurate approach on the mechanical properties of the standard photo-curable resin supplied by Anycubic inc. and the subsequent analysis to check the possibility of the resin to be used as a matrix for carbon nanotubes CNT's and copper nano particles CNP's. In order to achieve this goal, several factors had to be taken into account such as resin properties, technology to be used for the printing process, printing parameters for UV sensitive resins, design of the test specimens according to international standards, traction tests, statistical analysis of the data, and micro structural properties of the cured part.

4.1. Raw material and Technology

The resin used in this study belongs to a series of resins from Anycubic known as "Standard colored UV resin" in their product catalogue [55]. The aqua-blue colored resin was available at the CCComposites laboratory, **Figure 9** shows the 1 Lt resin presentation. The properties of this resin are reported on **Table 9** by the supplier.

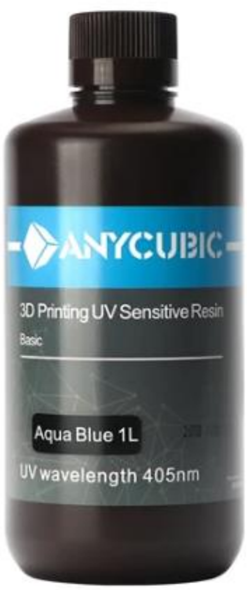

Figure 9. Aqua-blue Anycubic resin.

Table 9. Reported properties by the supplier.

Feature	value
Solidify wavelength	405nm
Shelf life	12 months
Hardness (D)	79.0
Viscosity@25°C	552 mpa.s
Liquid density	1.100 g/cm³
Solid Density	1.184 g/cm³
Tensile Strength	23.4 Mpa
Elongation	14.20%
Bottom exposure	20-60 s
Normal exposure	5-15 s

This resin, as many of its type, is a mixture of monomers, acrylates and polymerization iniciators, it has to be handled carefully, the composition reported by the *Newbest Testing Service* NTS is presented in **Table 10**. This testing service company released a safety datasheet of the resin that can be found in the following link:

https://fepfilm.eu/pobieranie/msds_anycubic_resin.pdf

Table 10. Basic composition of *Anycubic* UV resins.

Substance	Conc. (%)
Polyurethane acrylate	30-60
Acrylate monomer	10-40
Photo-initiator	10-5

Some of the safety issues of these resins include skin and eye contact hazard, breathing hazard, among others, therefore, the use of a mask and solvent resistant gloves is strongly required.

For the printing of the test specimens the ***photon*** LCD printer by ***Anycubic*** was used and it is depicted in **Figure 10**. This 3D printer is advertised on its website as being a SLA printer, which stands for Stereolithography apparatus, however, in the analysis of this work, we will explain why this device is not a SLA printer. Some specifications about the machine can be found in **Table 11**.

Table 11. Photon device specifications.

Technique	LCD shadow masking
Light source	UV-LED (405nm wavelength)
XY Resolution	0.047mm
Z axis accuracy	0.00125mm
Sug layer thickness	0.01 - 0.02 mm
Sug print speed	20mm/h
Rated power	40W
Build volume	115L * 65W * 155H (mm)

Figure 10. Photon LCD printer by Anycubic.

4.2. Test specimen design

A test specimen with general specifications for polymers [56] was designed initially as a photo-cured resin is considered a thermo-stable, rigid polymer. Rigid plastic analysis makes use of the assumption that the elastic deformation is so small that it can be ignored. Therefore, in using this method of analysis, the material behaves as if the structure does not deform until it collapses plastically [57].

Type I specimen was rejected as viable test specimen as its maximum measurement exceeded the print area of the 3D printer and print times exceeded 60 hours. As ASTM suggests [56], type V specimens shall be used when less material is available for evaluation, so the type V specimen was selected for this work. **Figure 11** shows the design created in ***Autodesk Inventor***, along with a sketch of its dimensions which were acquired from DIN638, testing methods for rigid and semi-rigid thermos-stable polymers.

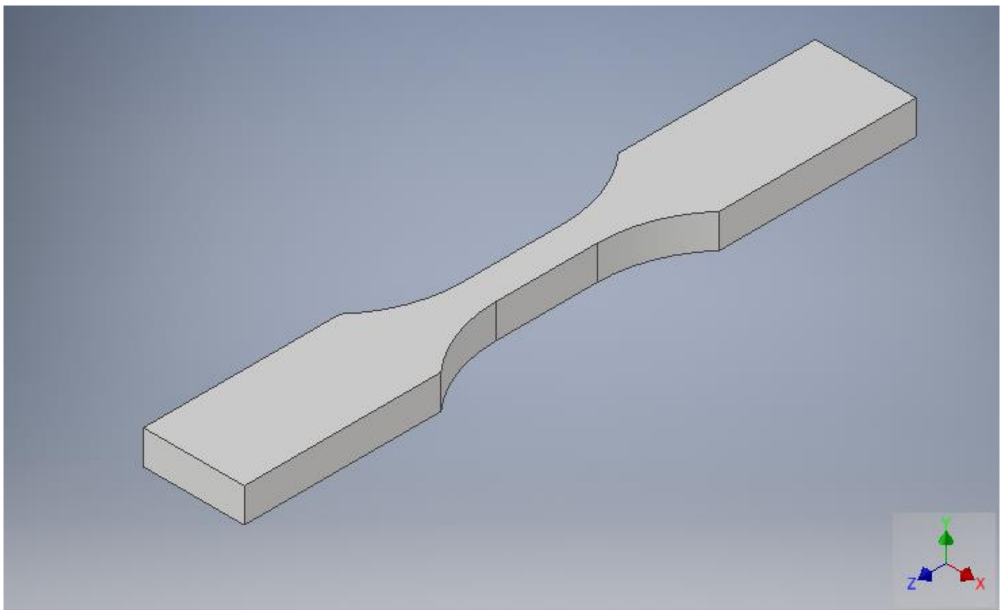

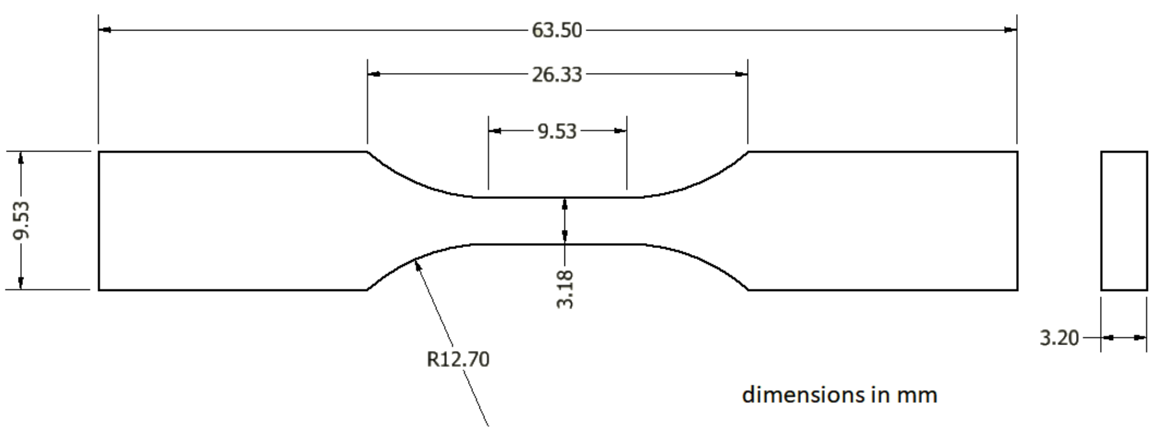

Figure 11. Test specimen designed in Inventor.

4.3. Printing parameters and specimen printing

In this 3DP technology there are several parameters involved related to the impression of the parts. The printing parameters to be taken into account are bottom exposure time, layer thickness, off time, number of bottom layers and normal exposure time. Since having a different exposure time in the initial layers would create a gradient of mechanical properties in the specimen, both the bottom exposure times and the bottom layer thickness were set to be the same values as those for normal exposure times and normal layer thickness. **Figure 12** shows an attempt to print the specimen with support material, this was not optimum as the supports left behind an indentation on the specimen surface. Therefore; these specimens were discharged.

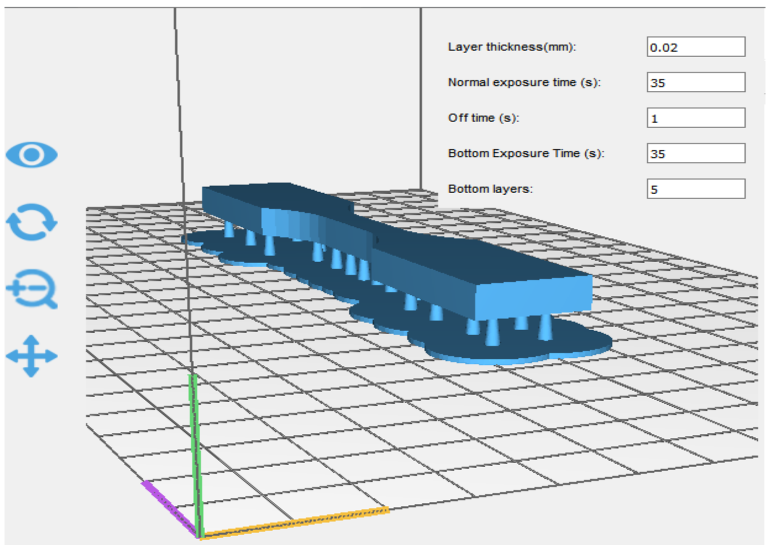

Figure 12. Supported specimen attempt.

10 type-V specimens were then printed with the parameters shown in **Figure 13Figure** ***14***, this parameters were obtained after a series of tries of failed printings, due to lack of cure time, or the layer thickness exceeding the cure depth. **Figure 14** shows a picture of the 10 printed specimens using the aqua-blue colored resin mentioned in 4.1.

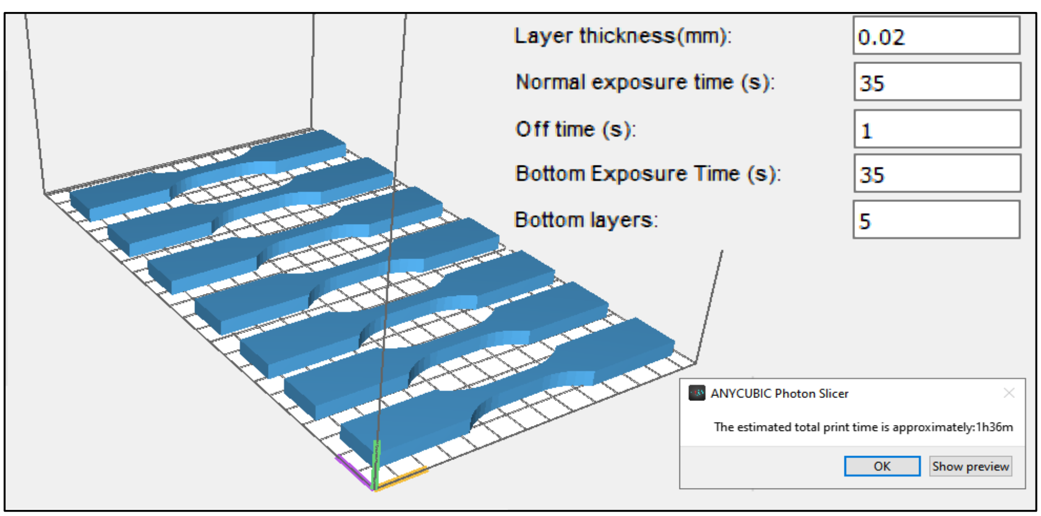

Figure 13. Final print parameters.

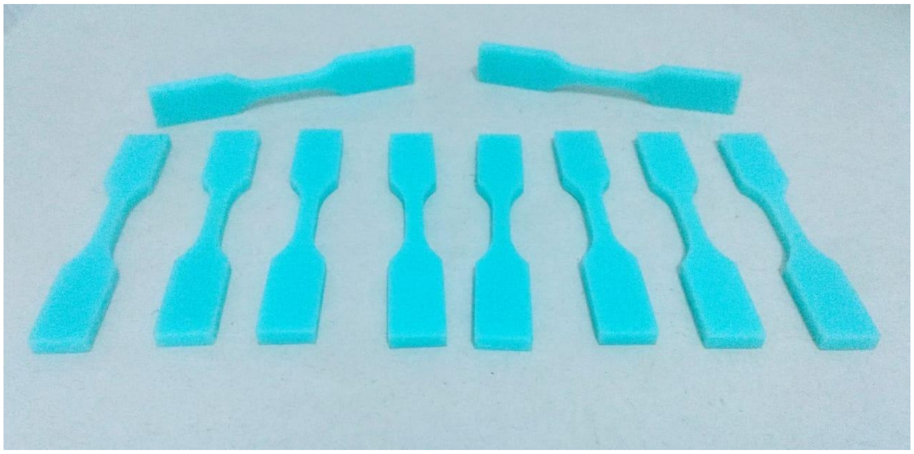

Figure 14. Final 3D printed specimens.

After the specimens were printed they have to go through a post-curing process as the polymerization process is not fully completed with this technology. There are several ways to finish this process, such as oven heating, UV light exposure through lamps and, if the geographical location receives a decent amount of sun radiation, then sun-light post-post curing is also acceptable. The printing time of the specimens was 1h 39m, 3 minutes more than the estimated by the software.

4.4. Destructive testing.

In order to obtain the Tensile strength of the cured parts, all of them were tested in the universal traction machine set up in Universidad de Antioquia facilities. Shows a picture of all the specimens after the traction test was performed. Data analysis and results will be discussed in the "analysis" chapter of this work.

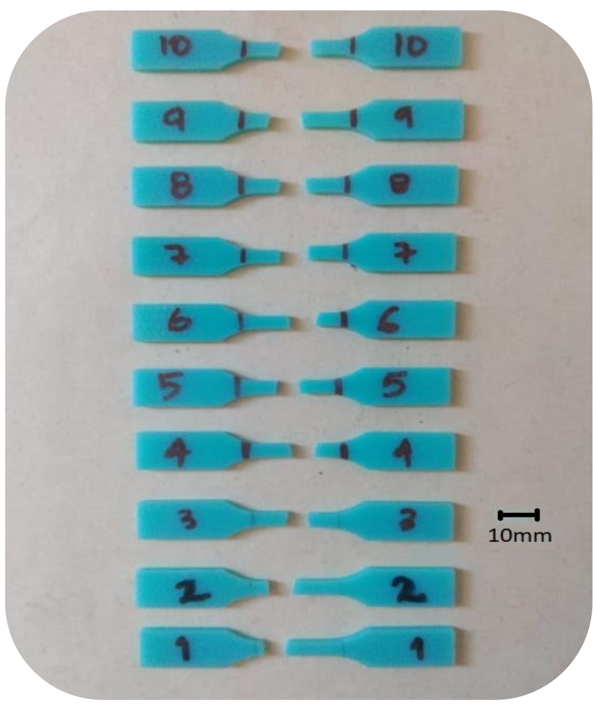

Figure 15. Test specimens after traction test.

4.5. Micro-structure

In order to test the maximum resolution of the device, a micro structural array was adopted and processed through Autodesk inventor mesh enabler. This micro structure has several symmetry planes, so this array was suitable to test the "voxel" resolution, which means the volumetric unit that the machine is able to print accurately.

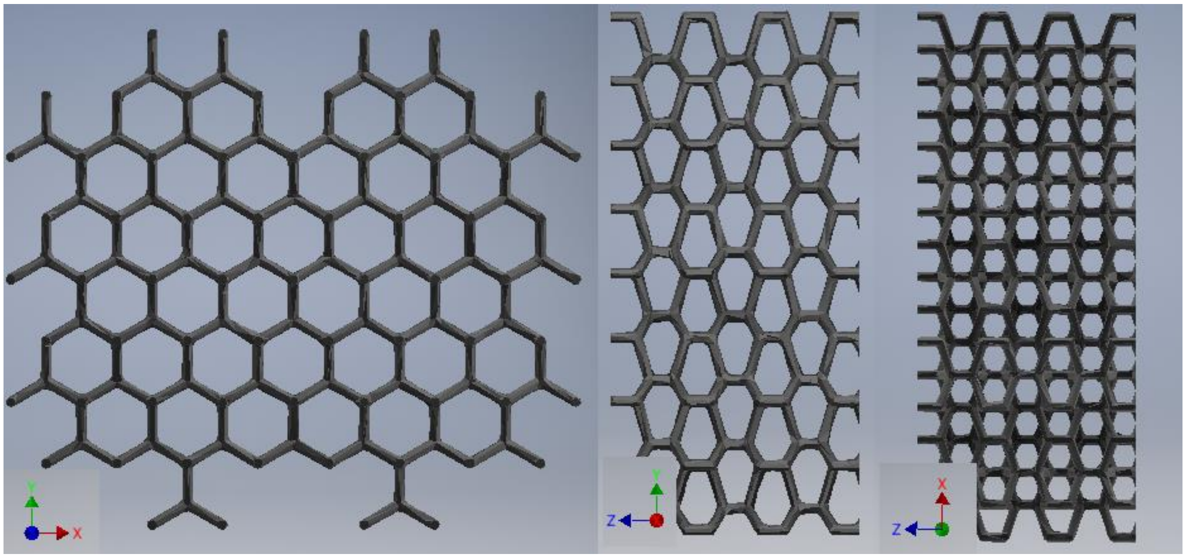

Figure 16. Modified and selected micro structure for printing with several symmetry planes.

The structure was then printed with the parameters shown in **Figure 17**.

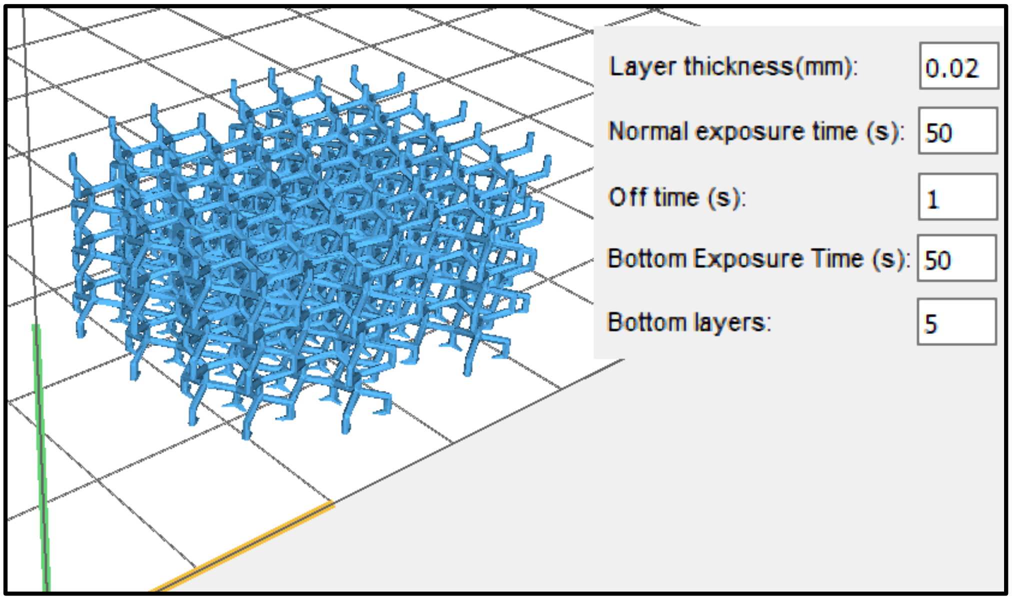

Figure 17. Printing parameters for the micro structure.

The results and analysis on the final result of the printing of the micro structure will be presented in a future segment of this work.

5. Results and analysis

In this section the results from the traction test will be discussed. Also a Weibull distribution is performed in order to obtain the Weibull modulus. A correlation analysis will also be performed in order to understand the importance of the printing parameters on the output variable, which is the tensile strength of the final cured part.

5.1. Strength vs Strain

One of the most relevant information that can be obtained from traction tests is the strength vs strain curve. As mentioned before, 10 specimens were tested and the results of this test are shown in **Table 12.** *Traction test results.* and with these values the Strength vs Strain curve can be obtained. **Figure 18** shows the beforementioned curve for 5 of the 10 specimens, even number (T-2, T-4, T-6, T-8, T-10) tests specimen results were plotted.

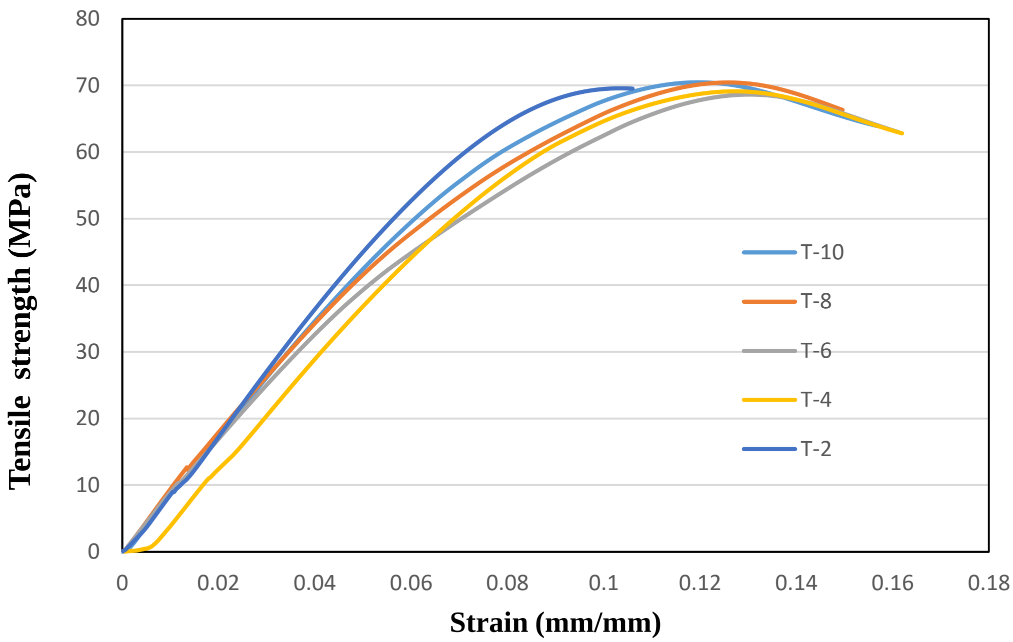

Figure 18. *Tensile strength vs Strain of test specimens 2-4-6-8-10.*

As the Tensile strength vs Strain graph is very similar on the tested specimens, a Weibull distribution is going to be used in order to analyze the variability of the data for both strain and strength and then will be compared for discussions. Also the tensile strength obtained in this work, as well as the strain, are going to be compared with the values given by the manufacturer and results will be discussed.

5.2. Weibull Modulus

In order to use a Weibull distribution, the results obtained from the traction tests must be used. **Table 12** presents both the maximum Strength and strain at failure for each of the 10 specimens.

Table 12. Traction test results.

Sample	Strength (Mpa)	Max strain
T-1	68.11	0.16
T-2	68.43	0.12
T-3	68.13	0.14
T-4	68.61	0.16
T-5	69.11	0.16
T-6	69.56	0.11
T-7	69.79	0.16
T-8	70.09	0.14
T-9	70.43	0.15
T-10	70.46	0.16
Median	69.33	0.15

The Weibull modulus is a dimensionless parameter obtained from a Weibull distribution that is used to describe the variability in measured material strength, hardness, strain, among other properties, of brittle or rigid materials. For this analysis a single-parameter Weibull distribution will be used to determine the Weibull modulus obtained by both the Strength and the strain. The parameter is calculated as follows.

$$P_f = 1 - e^{\left(\frac{-\sigma_f}{\sigma_0}\right)^m} \qquad (5.1)$$

Where P_f is the probability of failure, σ_f is the strength at failure, σ_0 is the scaling parameter, and m is the Weibull Modulus.

Equation 5.2 is obtained after applying some mathematical treatment to equation 5.1.

$$\ln\left(ln\left(\frac{1}{1-P_f}\right)\right) = m \ln \sigma_f - m \ln \sigma_0 \qquad (5.2)$$

This is the linearized form of equation 5.1, which allows us to extract the Weibull module (m) from the collected data. As equation 5.2 has the form of $y = mx - b$, with m (Weibull module) being the slope of the tendency line from the distribution. The failure probability of the specimens was calculated as follows.

$$P_f = j/(r+1) \qquad (5.3)$$

Where j is the rank of the data and r is the number of total tested specimens, a plot of this Failure probability vs the Strength at failure is shown in **Figure 19-A**. Failure probability vs Strain is shown in **Figure 18-C**. Using these failure probabilities, we then find a Weibull probability, which is the left side of equation 5.2, and then plot it against the natural log of the strength at failure. Then the equation of the trend line generated directly gives the value of Weibull module for this data distribution. The equations obtained from **Figure 18-B** and **Figure 18-D** are:

Weibull regression for Strength $\boldsymbol{y = 72.588x - 308.12}$ (5.4)

Weibull regression for Strain $\boldsymbol{y = 6.849x + 12.789}$ (5.5)

Then, the Weibull module obtained from Strength data is $\boldsymbol{m_{strength} = 75.588}$, and the one obtained from Strain data is $\boldsymbol{m_{strain} = 6.849}$. The R^2 values from both Strength and Strain based distributions are 0.9213 and 0.9273 respectively, and they are an indicator that a Weibull distribution is a good fit for the obtained data.

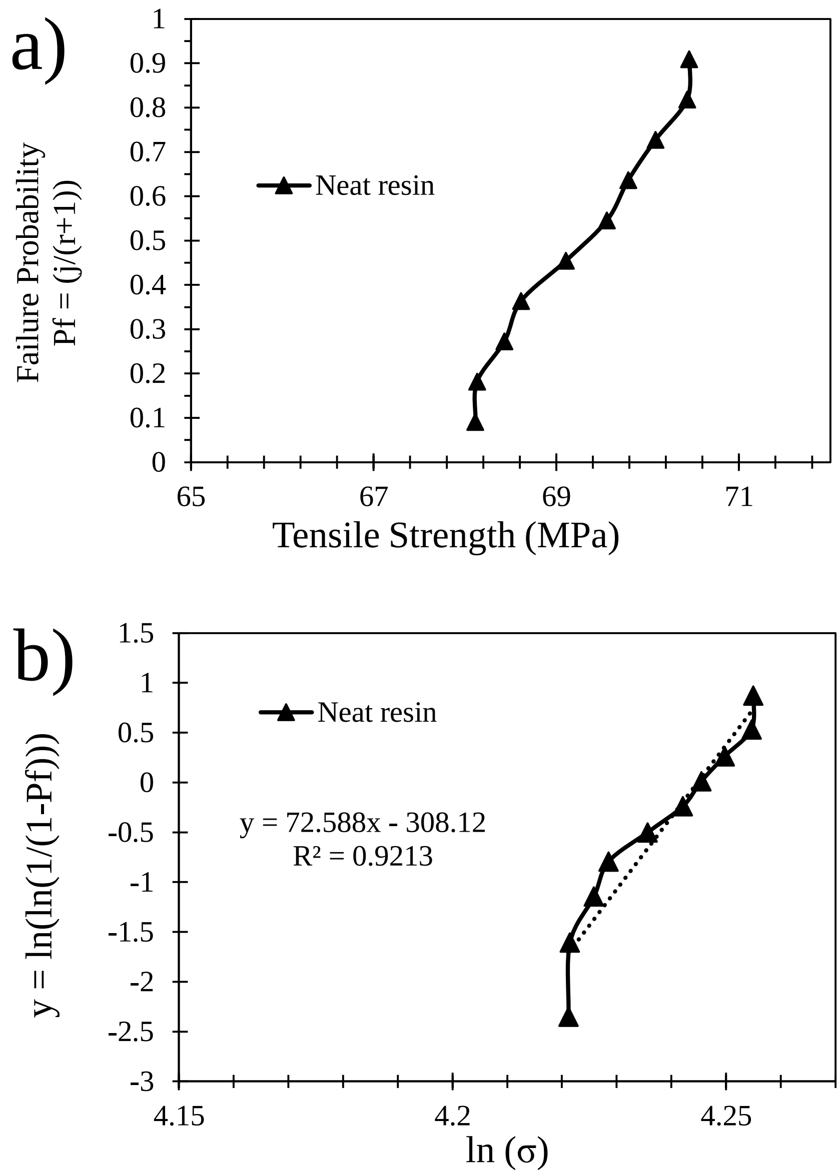

Figure 19. a) Failure probability vs Strength at failure.
b) Weibull probability vs ln of strength at failure.

The higher the Weibull modulus is, the more consistent the material is, which means that uniform "defects" are evenly distributed throughout the entire volume. Also, a high Weibull module is an indicator of how narrow the probability curve of the strength distribution is. Usual values of Weibull modules go from 10 to 20 [58]. Therefore, the obtained Weibull module for this work is a good indicator of the collected data from the Tensile strength test of this 3D-printed UV resin.

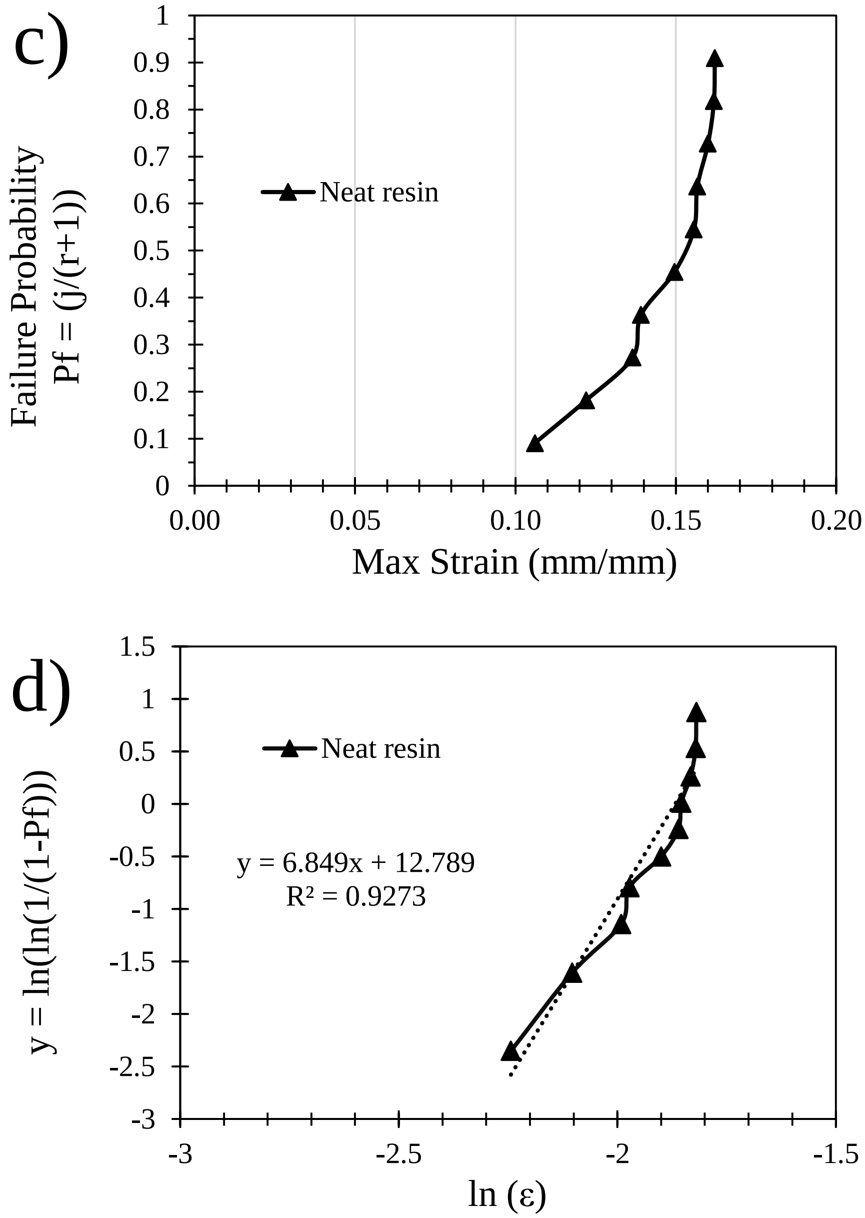

Figure 19. **c)** Failure probability vs maximum Strain.
d) Weibull probability vs ln of max Strain

6. Discussion

In this section of the work the results from the traction tests, the Weibull modulus and the printed micro structure will be discussed.

6.1. Property comparison

Anycubic inc, the manufacturer company of the resin used for this study, supplied several properties from the studied UV colored resin, a comparison of those properties is performed here.

Using the suggested printing parameters from the supplier **(Table 9)**, they reported the Tensile Strength to be 23.4 Mpa, and an elongation of 14.20%. The Tensile Strength obtained in this work by changing the printing parameters was that of 69.3 Mpa, which is 2.96 times the advertised value.

The mean elongation of the 10 test specimens is calculated as follows.

$$\bar{\delta} = \bar{\varepsilon} * L = 0.15 * 63.5 = 9.525 \qquad (6.1)$$

Therefore, the obtained elongation given by the manufacturer is higher than the obtained in the tests, representing a decrease in elongation of 4.675%. The decrease in elongation indicates that the final cured test specimens with the printing parameters used in the study are more rigid. Nevertheless, they show a higher Tensile strength.

6.2. Weibull Modulus comparison

Two different Weibull Modules were calculated in this study, one obtained from the Strength data and another from Strain. Both modulus are frequently used in statistical approaches for brittle materials [59]. The Weibull module obtained from Strength data was 75.588 whereas the one obtained from strain data was 6.849. As a higher Weibull module indicates a better and narrower distribution of the data, the Weibull modulus obtained from Strength data then displays a more reliable set of data to obtain information from.

The Weibull modulus obtained from Strain data, then is a less reliable source of statistical information, meaning that the mean Strength obtained from the Traction test is a more reliable datum than the mean Strain.

6.3. Micro structure results

The proposed micro structure was successfully printed in the machine with a very high resolution. **Figure 21** shows the final printed micro structure compared with a 500-Colombian peso coin.

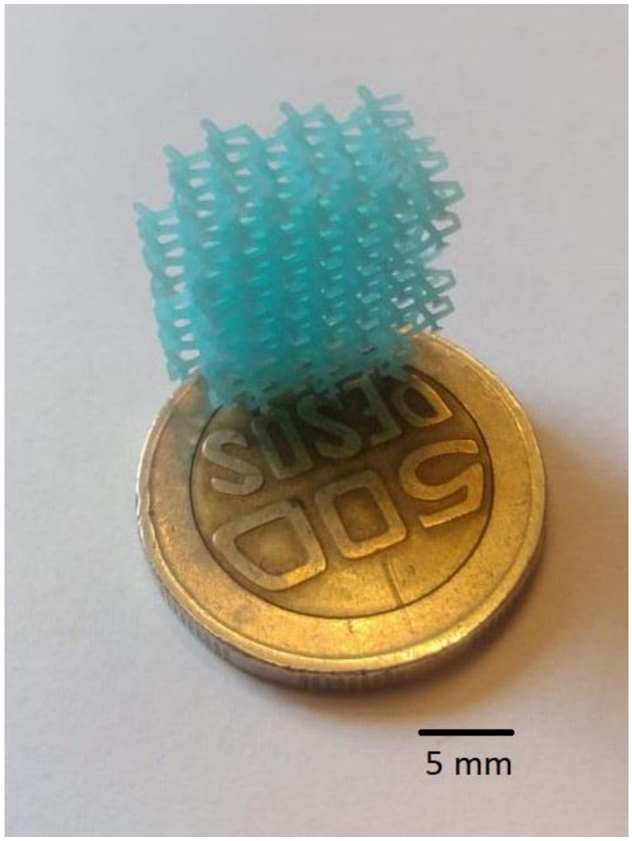

Figure 20. Micro Structure printed in the Photon device.

A printing of the cross section of the microstructure was made in different sizes in order to find out the best resolution to print the micro structure, such printing is depicted in **Figure 22.**

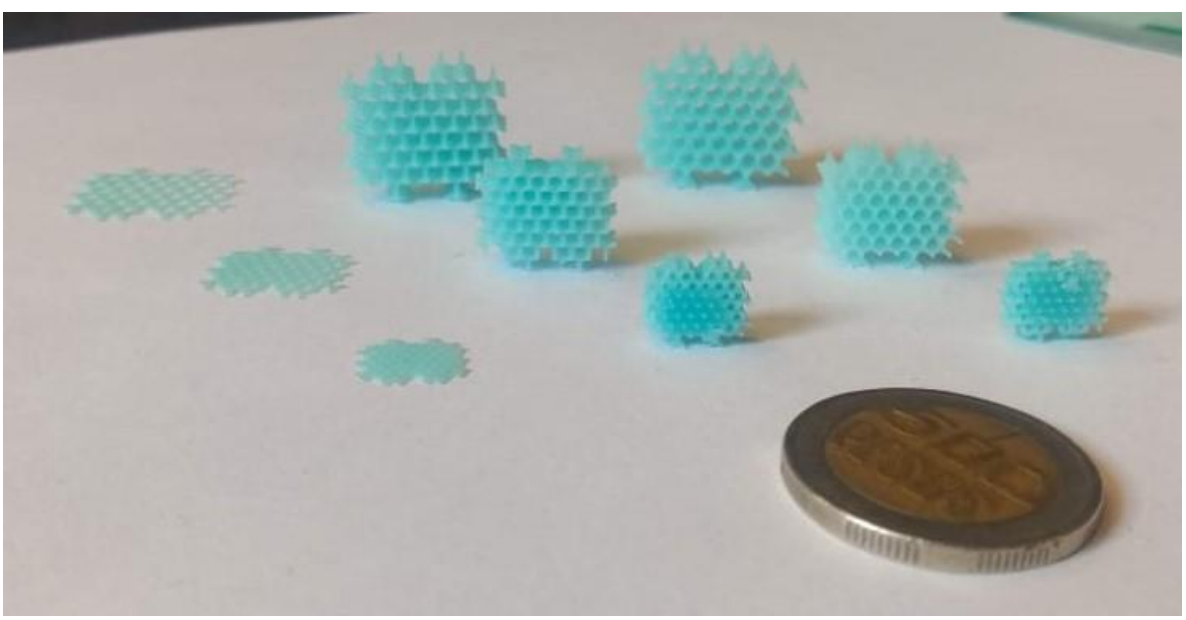

Figure 21. Micro structures and their respective cross sections.

The resolution obtained in the microstructures allows this work to open up a series of opportunities for micro fabrication and manufacture of nanocomposites. As this technology is now easy to access, this may increase the number of application fields of DLP, SLA and LCD printed parts.

For instance, a future work can be done by studying the behavior of this resins when adding Carbon Nano Tubes (CNT's) or copper Nano particles (CNP's), and by using biodegradable resins, applications can go from biomedical implants to environmentally friendly impact absorbers.

If a compression test shows good results on these microstructures, then they can be filled with piezo-electric materials in order to obtain a new type of piezo electric response to be used in a wide range of fields.

7. Conclusions

Tensile Strength of the Anycubic colored resin was confirmed in this work. In addition, an increase on this property of 2.96 times was achieved by changing the printing parameters of layer thickness and UV exposure times.

Anycubic inc. advertises the Photon machine as a "SLA" Stereolithography apparatus, but according to the systematic review performed in this work, the technology that the machine uses is not that of Stereolithography, but rather a shadow masking of a UV-led display, which allows the curing process of a complete layer, offering faster printing times but not such as good resolution of a SLA.

Weibull modulus were obtained from both sets of data Strength and Strain, showing that a Tensile Strength based modulus is a more reliable collection of data for this type of material. Weibull modulus were both greater than 0 which indicates that the probability of failure increases with time.

This technology will enable the possibility of manufacturing new composite materials with nano reinforcements, due to the good printing resolution obtained by the printing of micro-structural array.

8. Supplementary information

Table 13. Matrix and Nano-reinforcement materials used in the studied articles, as well as the pre and post processing used.

ref	Matrix	Filler	enhancements	pre-processing	post-processing
[23]	Form Clear v2 (acrylic monomers and oligomers)	GNP (avanGRP-40)	Young's Modulus	high-shear mixing, degassification	IPA wash, 60°C heating, UV post-cure
[24]	highly hydrated polymer	NR	continuous printing	oxygen-permeable build window	NR
[25]	methacrylic acid (MA) resin	Cellulose Nano-crystals	strength, thermal stability	ultra-sonication, freeze drying, grinding	160°C heating, UV post-cure
[26]	methacrylic acid (MA) resin	Graphene Oxide	Tensile strength, ductility	synthetized Graphene oxide, grinding	IPA wash, 60°C heating, UV post-cure
[27]	polyurethane acrylate-based resin	Cellulose Nano-fibrils	Tensile strength	cellulose surface PEG treatment	IPA wash, UV post-cure
[28]	polymethyl-methacrylic resin (Tethon 3D)	graphene, carbonyl iron	Tensile strength, thermal conductivity	electro-chemical exfoliation	EtOH 99% wash, UV post-cure
[29]	acrylic resin (Ebecryl 7100)	silver salt (AgNP's)	Tensile strength, ductility	overnight mixing of resin and Ag-Salt	IPA wash, thermal post-cure @90°C
[30]	acrylic resin (FLGPGRO2)	Graphene Oxide	Stiffness, Tensile strength	acetone-sonication, mixture ultrasonication	IPA wash, mild annealing @50°C & 100°C
[31]	Poly(ethylene glycol) diacrylate (PEGDA575) based hydrogel	Cellulose Nano-crystals	Tensile strength, ductility	mixture ultrasonication	phosphate-buffered saline (PBS) wash
[32]	PTMC-MA resin and PTMC-MA/nHA resins (custom mix)	hydroxyapatite Nano-crystals	Tensile strength, E modulus	Cold-Methanol precipitation, stirring	propylene carbonate/ethanol wash

9. Acknowledgments

Author acknowledges the Vicerrectoría de Extensión from Universidad de Antioquia for sponsoring this research work through the project ASCON19-493. I also thank Henry Alonso Colorado Ph.D. for his mentoring throughout this work.

10. References

[1] I. Gibson, D. Rosen, B. Stucker, Additive Manufacturing Tech- nologies, Springer, NY, USA 2010.

[2] A. Medellin, W. Du, G. Miao, J. Zou, Z. Pei, and C. Ma, "Vat photopolymerization 3d printing of nanocomposites: A literature review," *J. Micro Nano-Manufacturing*, vol. 7, no. 3, 2019, doi: 10.1115/1.4044288.

[3] ASTM, 2015, 'Standard Terminology for Additive Manufacturing—General Principles—Terminology,' ASTM International. West Conshohocken, PA, Standard No. ISO/ASTM52900-15.

[4] PWC, http://www.pwc.com/us/en/industrial-products/assets/ 3d-printing-next_manufacturing-chart-pack-pwc.pdf (accessed: April 2016).

[5] https://formlabs.com/blog/resin-3d-printer-comparison-sla-vs-dlp/.

[6] Melchels, F. P., Feijen, J., and Grijpma, D. W., 2010, 'A Review on Stereoli- thography and Its Applications in Biomedical Engineering,' Biomaterials, 31(24), pp. 6121–6130.

[7] M. D. B. Fabio Ganovelli, Massimiliano Corsini,Sumanta Pattanaik, *Introduction to Computer Graphics: A Practical Learning Approach*. 2015.

[8] Farahani, R.D.; Dub, M.; Therriault, D. Three-Dimensional Printing of Multifunctional Nanocomposites: Manufacturing Techniques and Applications. Adv. Mater. 2016, 28, 5794–5821.

[9] Yuanyuan, Z.; Houmin, L.; Xi, Y.; Tao, Z.; Kaiqiang, Z.; Wei, S.Z.L.; Sun, H. Additive Manufacturing of Carbon Nanotube-Photopolymer Composite Radar Absorbing Materials. Polym. Compos. 2016.

[10] Kim, K.; Zhu, W.; Qu, X.; Aaronson, C.; McCall, W.R.; Chen, S.C.; Sirbuly, D.J. 3D optical printing of piezoelectric nanoparticle—Polymer composite materials. ACS Nano 2014, 8, 9799–9806.

[11] A. Morelli, D. Puppi, and F. Chiellini, "Polymers from renewable resources: Perspectives in biomedical applications," *J. Renew. Mater.*, vol. 1, no. 2, pp. 83–112, 2013, doi: 10.7569/JRM.2012.634106.

[12] Matsuhisa, N.; Inoue, D.; Zalar, P.; Jin, H.; Matsuba, Y.; Itoh, A.; Yokota, T.; Hashizume, D.; Someya, T. Printable elastic conductors by in situ formation of silver nanoparticles from silver flakes. Nat. Mater. 2017, 16, 834–840.

[13] P. Rastogi and B. Kandasubramanian, "Breakthrough in the printing tactics for stimuli-responsive materials: 4D printing," *Chem. Eng. J.*, vol. 366, no. November 2018, pp. 264–304, 2019, doi: 10.1016/j.cej.2019.02.085.

[14] M. Petroff *et al.*, "A 3D-printed broadband millimeter wave absorber," Aug. 2018, doi:

10.1063/1.5050781.

[15] H. Cui *et al.*, “Three-dimensional printing of piezoelectric materials with designed anisotropy and directional response,” *Nat. Mater.*, vol. 18, no. 3, pp. 234–241, Mar. 2019, doi: 10.1038/s41563-018-0268-1.

[16] https://3dprint.com/133158/3d-printable-bones/.

[17] https://3dprintingindustry.com/wp-content/uploads/2017/01/maxresdefault-1-e1483701139912.jpg.

[18] https://www.anycubic.com/pages/about-anycubic.

[19] A. Paesano, “Polymers for additive manufacturing: Present and future,” *SAMPE J.*, vol. 50, no. 5, pp. 34–43, 2014.

[20] P.-H. Lee, H. Chung, S. W. Lee, J. Yoo, and J. Ko, “Review: Dimensional accuracy in additive manufacturing processes,” in *ASME 2014 International Manufacturing Science and Engineering Conference, MSEC 2014 Collocated with the JSME 2014 International Conference on Materials and Processing and the 42nd North American Manufacturing Research Conference*, 2014, vol. 1, doi: 10.1115/MSEC2014-4037.

[21] J. Deckers, J. Vleugels, and J.-P. Kruth, “Additive manufacturing of ceramics: A review,” *J. Ceram. Sci. Technol.*, vol. 5, no. 4, pp. 245–260, 2014, doi: 10.4416/JCST2014-00032.

[22] P. M. Dickens, “Research Developments in Rapid Prototyping,” *Proc. Inst. Mech. Eng. Part B J. Eng. Manuf.*, vol. 209, no. 4, pp. 261–266, 1995, doi: 10.1243/PIME_PROC_1995_209_082_02.

[23] A. S. De León and S. I. Molina, “Influence of the degree of cure in the bulk properties of graphite nanoplatelets nanocomposites printed via stereolithography,” *Polymers (Basel).*, vol. 12, no. 5, 2020, doi: 10.3390/POLYM12051103.

[24] J. Li, C. Wu, P. K. Chu, and M. Gelinsky, “3D printing of hydrogels: Rational design strategies and emerging biomedical applications,” *Mater. Sci. Eng. R Reports*, vol. 140, no. January, p. 100543, 2020, doi: 10.1016/j.mser.2020.100543.

[25] B. Wang *et al.*, “A physical and chemical double enhancement strategy for 3D printing of cellulose reinforced nanocomposite,” *J. Appl. Polym. Sci.*, no. August 2019, pp. 1–11, 2020, doi: 10.1002/app.49164.

[26] J. O. Palaganas, N. B. Palaganas, L. J. I. Ramos, and C. P. C. David, “3D Printing of Covalent Functionalized Graphene Oxide Nanocomposite via Stereolithography,” *ACS Appl. Mater. Interfaces*, vol. 11, no. 49, pp. 46034–46043, 2019, doi: 10.1021/acsami.9b12071.

[27] D. Mohan, M. S. Sajab, H. Kaco, S. B. Bakarudin, and A. M. Noor, “3D Printing of Uv-Curable Polyurethane Incorporated With Surface-Grafted Nanocellulose,” *Nanomaterials*, vol. 9, no. 12, 2019, doi: 10.3390/nano9121726.

[28] Y. Zuo, Z. Yao, H. Lin, J. Zhou, J. Lu, and J. Ding, “Digital light processing 3D printing of graphene/carbonyl iron/polymethyl methacrylate nanocomposites for efficient microwave absorption,” *Compos. Part B Eng.*, vol. 179, p. 107533, 2019, doi: 10.1016/j.compositesb.2019.107533.

[29] G. Taormina, C. Sciancalepore, F. Bondioli, and M. Messori, “Special resins for stereolithography: In situ generation of silver nanoparticles,” *Polymers (Basel).*, vol. 10, no.

2, 2018, doi: 10.3390/polym10020212.

[30] J. Z. Manapat, J. D. Mangadlao, B. D. B. Tiu, G. C. Tritchler, and R. C. Advincula, “High-Strength Stereolithographic 3D Printed Nanocomposites: Graphene Oxide Metastability,” *ACS Appl. Mater. Interfaces*, vol. 9, no. 11, pp. 10085–10093, 2017, doi: 10.1021/acsami.6b16174.

[31] N. B. Palaganas *et al.*, “3D printing of photocurable cellulose nanocrystal composite for fabrication of complex architectures via stereolithography,” *ACS Appl. Mater. Interfaces*, vol. 9, no. 39, pp. 34314–34324, 2017, doi: 10.1021/acsami.7b09223.

[32] M. A. Geven *et al.*, “Fabrication of patient specific composite orbital floor implants by stereolithography,” *Polym. Adv. Technol.*, vol. 26, no. 12, pp. 1433–1438, 2015, doi: 10.1002/pat.3589.

[33] J. Z. Manapat, Q. Chen, P. Ye, and R. C. Advincula, “3D Printing of Polymer Nanocomposites via Stereolithography,” *Macromol. Mater. Eng.*, vol. 302, no. 9, pp. 1–13, 2017, doi: 10.1002/mame.201600553.

[34] Feng, X., Yang, Z., Chmely, S., Wang, Q., Wang, S., and Xie, Y., 2017, ‘Lignin-Coated Cellulose Nanocrystal Filled Methacrylate Composites Pre- pared Via 3D Stereolithography Printing: Mechanical Reinforcement and Ther- mal Stabilization,’ Carbohydr. Poly.

[35] Gurr, M., Thomann, Y., Nedelcu, M., K€ubler, R., K€oncz€ol, L., and M€ulhaupt, R., 2010, “Novel Acrylic Nanocomposites Containing In-Situ Formed Calcium Phosphate/Layered Silicate Hybrid Nanoparticles for Photochemical Rapid Pro- totyping, Rapid Tooling a.

[36] https://www.desktopmachinery.com/wp-content/uploads/2018/10/3DP-Cure-01_website_image-e7361ead-fc70-43e7-a2eb-f5f2a8f2a402.jpg.

[37] S. Mubarak *et al.*, “Enhanced mechanical and thermal properties of stereolithography 3d printed structures by the effects of incorporated controllably annealed anatase TiO2 nanoparticles,” *Nanomaterials*, vol. 10, no. 1, 2020, doi: 10.3390/nano10010079.

[38] H. Wu *et al.*, “Recent developments in polymers/polymer nanocomposites for additive manufacturing,” *Prog. Mater. Sci.*, vol. 111, no. April 2019, 2020, doi: 10.1016/j.pmatsci.2020.100638.

[39] Z. Feng *et al.*, “Graphene-reinforced biodegradable resin composites for stereolithographic 3D printing of bone structure scaffolds,” *J. Nanomater.*, vol. 2019, 2019, doi: 10.1155/2019/9710264.

[40] J. R. C. Dizon, A. H. Espera, Q. Chen, and R. C. Advincula, “Mechanical characterization of 3D-printed polymers,” *Addit. Manuf.*, vol. 20, pp. 44–67, 2018, doi: 10.1016/j.addma.2017.12.002.

[41] S. Mubarak *et al.*, “Enhanced mechanical and thermal properties of stereolithography 3d printed structures by the effects of incorporated controllably annealed anatase TiO<inf>2</inf> nanoparticles,” *Nanomaterials*, vol. 10, no. 1, 2020, doi: 10.3390/nano10010079.

[42] Küpper D, Heising W, Corman G, Wolfgang M, Knizek C, Lukic V. Get ready for industrialized additive manufacturing. Digital, BCG, Boston Consulting Group; 2017.

[43] https://all3dp.com/1/wanhao-duplicator-7-d7-plus-3d-printer-review/.

[44] https://www.aniwaa.com/product/3d-printers/envisiontec-perfactory-3-mini-multi-lens/.

[45] https://archive-media.formlabs.com/upload/Form-1-plus-overview-US.pdf.

[46] https://www.aniwaa.com/product/3d-printers/formlabs-form1-2/.

[47] https://all3dp.com/formlabs-form-2-review-price-sla-3d-printer/.

[48] https://www.anycubic.com/products/anycubic-photon-3d-printer.

[49] E. L. Jeroen B. Guinée, *Handbook on Life Cycle Assessment: Operational Guide to the ISO Standards*. Kluwer Academic Publishers, 2004.

[50] A. Zhakeyev, P. Wang, L. Zhang, W. Shu, H. Wang, and J. Xuan, "Additive Manufacturing: Unlocking the Evolution of Energy Materials," *Adv. Sci.*, vol. 4, no. 10, 2017, doi: 10.1002/advs.201700187.

[51] H. A. Balogun, R. Sulaiman, S. S. Marzouk, A. Giwa, and S. W. Hasan, "3D printing and surface imprinting technologies for water treatment: A review," *J. Water Process Eng.*, vol. 31, 2019, doi: 10.1016/j.jwpe.2019.100786.

[52] C. Bressot *et al.*, "Sanding and analysis of dust from nano-silica filled composite resins for stereolithography," *Chem. Eng. Res. Des.*, vol. 156, pp. 23–30, 2020, doi: 10.1016/j.cherd.2020.01.011.

[53] M. R. Khosravani and T. Reinicke, "On the environmental impacts of 3D printing technology," *Appl. Mater. Today*, vol. 20, 2020, doi: 10.1016/j.apmt.2020.100689.

[54] H. A. Balogun, R. Sulaiman, S. S. Marzouk, A. Giwa, and S. W. Hasan, "3D printing and surface imprinting technologies for water treatment: A review," *J. Water Process Eng.*, vol. 31, no. October 2018, p. 100786, 2019, doi: 10.1016/j.jwpe.2019.100786.

[55] https://www.anycubic.com/collections/uv-resin/products/colored-uv-resin-for-photon-series?variant=30151434895420.

[56] ASTM, "Standard Test Method for Tensile Properties of Plastics." 2014.

[57] M. B. Wong, "Manual Methods of Plastic Analysis," in *Plastic Analysis and Design of Steel Structures*, Elsevier, 2009, pp. 139–162.

[58] http://www.keramverband.de/brevier_engl/5/3/3/5_3_3_4.htm#:~:text=The%20higher%20the%20Weibull%20modulus,curve%20of%20the%20strength%20distribution

[59] P. Forquin and F. Hild, "A Probabilistic Damage Model of the Dynamic Fragmentation Process in Brittle Materials," 2010, pp. 1–72.

List of Tables

List of figures